

# Lévy Ratchet in a Weak Noise Limit: Theory and Simulation

I. Pavlyukevich<sup>1,a</sup>, B. Dybiec<sup>2,b</sup>, A. V. Chechkin<sup>3,c</sup>, and I. M. Sokolov<sup>4,d</sup>

<sup>1</sup> Institut für Stochastik, Friedrich–Schiller–Universität Jena, Ernst–Abbe–Platz 2, 07743 Jena, Germany

<sup>2</sup> M. Smoluchowski Institute of Physics, and M. Kac Center for Complex Systems Research, Jagellonian University, ul. Reymonta 4, 30–059 Kraków, Poland

<sup>3</sup> School of Chemistry, Tel Aviv University, Ramat Aviv, Tel Aviv 69978, Israel and Institute for Theoretical Physics NSC KIPT, Akademicheskaya st. 1, Kharkov 61108, Ukraine

<sup>4</sup> Institut für Physik, Humboldt–Universität zu Berlin, Newtonstrasse 15, 12489 Berlin, Germany

**Abstract.** We study the motion of a particle embedded in a time independent periodic potential with broken mirror symmetry and subjected to a Lévy noise possessing Lévy stable probability law (Lévy ratchet). We develop analytical approach to the problem based on the asymptotic probabilistic method of decomposition proposed by P. Imkeller and I. Pavlyukevich [J. Phys. A **39**, L237 (2006); Stoch. Proc. Appl. **116**, 611 (2006)]. We derive analytical expressions for the quantities characterizing the particle motion, namely the splitting probabilities of first escape from a single well, the transition probabilities and the particle current. A particular attention is devoted to the interplay between the asymmetry of the ratchet potential and the asymmetry (skewness) of the Lévy noise. Intensive numerical simulations demonstrate a good agreement with the analytical predictions for sufficiently small intensities of the Lévy noise driving the particle.

## 1 Introduction

Lévy motion, also referred to as “Lévy flights”, stands for a class of non-Gaussian Markovian random processes whose stationary increments are distributed according to the Lévy stable probability laws originally studied by French mathematician Paul Pierre Lévy [1]. The term “Lévy flights” (LF) was coined by Mandelbrot [2], who thus poeticized this type of random motion which is now considered as a paradigm of non-Brownian random walk. Similar to Brownian motion, LFs have a solid probabilistic background. Indeed, the central limit theorem and the properties of Gaussian probability laws and processes constitute mathematical foundation of the Brownian motion [3]. At the same time, the *generalized* central limit theorem and the remarkable properties of the Lévy stable probability laws serve as the basis of the LFs theory. Generalized central limit theorem says that the stable probability laws, like the Gaussian law, attract the distributions of sums of random variables [4]. Due to this reason, Lévy stable distributions naturally appear when evolution of a system, or result of an experiment are determined by the sum of independent, identically distributed random factors. The probability density functions (PDFs) of the stable laws exhibit slowly decaying, power-law asymptotic behavior of the form  $|x|^{-(1+\alpha)}$ , where  $\alpha$  is called the Lévy index,  $0 < \alpha < 2$ . Due to this reason

---

<sup>a</sup> e-mail: ilya.pavlyukevich@uni-jena.de

<sup>b</sup> e-mail: bartek@th.if.uj.edu.pl

<sup>c</sup> e-mail: achechkin@kipt.kharkov.ua

<sup>d</sup> e-mail: igor.sokolov@physik.hu-berlin.de

the stable PDFs appear naturally in the description of random processes with large outliers, far from equilibrium. Another important property of LFs is their statistical self-similarity, or self-affinity [5]. Therefore, like the Brownian motion, they are naturally suited for the description of random fractal processes. LFs are ubiquitous in nature and they were observed in various fields of science, including physics (stochastic dynamics, turbulent flows [6,7,8,9], turbulence and turbulent transport in magnetized plasmas [10,11,12,13], optical lattices [14], molecular collisions [15]), biology (heartbeat dynamics [16], firing of neural networks [17], searching on a folding polymer [18], foraging movement [19]), seismology (recording of seismic activity [20]), stochastic climate dynamics [21], engineering (signal processing [22,23,24]), economics (financial time series [25,26,27]), and even the spreading of diseases and dispersal of banknotes [28]. The list above is far from being complete; we only mention that recently illuminating experiments with LFs of light have been reported [29,30].

The behavior of LFs in external fields brings a few surprising effects. The PDF in a harmonic potential evolves to a stationary state given by a Lévy stable distribution [31,32] with the same stability index  $\alpha$  as the underlying noise. For unimodal power law potentials steeper than a harmonic one  $U(x) \propto |x|^c$ ,  $c > 2$ , the stationary state is characterized by the asymptotic power law decay,  $p(x) \propto |x|^{-(c+\alpha-1)}$ . These stationary probability densities decay faster [33,34,35,36] than the corresponding Lévy stable density. Moreover, the stationary PDFs in such potentials are bimodal, i.e. they possess a local minimum at the origin and two maxima at  $x \neq 0$ . The study of unimodal to multimodal bifurcations in this system during relaxation was addressed in Ref. [37,38,39]. For subharmonic potential  $c < 2$  the decay  $p(x) \propto |x|^{-(c+\alpha-1)}$  is slower than the decay of the corresponding Lévy stable density. Moreover, stationary states only exist for  $c > 2 - \alpha$  [40].

The properties of the LFs in external fields were studied with the use of space-fractional Fokker-Planck equation and the Langevin equation for a particle driven by Lévy noise. Motivated by the model from stochastic climate dynamics [21], the barrier crossing problem for LFs in generic types of the potentials was studied in Refs. [41,42,43,44,45,46]. In particular, the method of decomposition of the Lévy process into bounded jump component and compound Poisson part proposed in Refs. [45,46] allowed for treating the escape problem analytically (at least in the weak noise asymptotics), while solving the corresponding space-fractional Fokker-Planck equation poses considerable difficulties [42]. Further, the idea of decomposition was applied to describe a metastable behavior of a multi-well dynamical system driven by Lévy noise [47]. This have led to a new approach to fast simulated annealing problem [48] of efficient non-local search of the deepest potential well [49,50]. We will discuss the decomposition method in more detail below, see Sec. 3.1.

Lévy processes lead to a richer behavior than Gaussian processes to which they reduce for  $\alpha = 2$ . Moreover the limiting distributions for sums of independent identically distributed random variables do not need to be symmetric. The asymmetry of the noise can induce preferred direction of the motion [51,52] and asymmetry of stationary states [53]. This in turn is responsible for occurrence of the dynamical hysteresis [54].

In this paper we study, both analytically and numerically, LFs in a ratchet potential, i.e. in a periodic potential lacking reflection symmetry. Such spatial symmetry breaking gives rise to a net directed transport in presence of non-equilibrium fluctuations. The motion in ratchet potentials attracted considerable attention due to its role in fluctuation-driven transport, see for example Ref. [55] and references therein. By now, the physics of “Brownian motors” is well understood and the theory is well developed. However, not too much is known about Lévy ratchets. In Ref. [56] the authors solved numerically the Langevin equation with a white Lévy noise for an overdamped particle in a ratchet potential. They demonstrated the appearance of directional transport using such measures of directionality as the position of the median of particle’s displacements distribution characterizing the group velocity, and the interquantile distance giving the distributions’ width. Such an approach allows the authors to study Lévy ratchet in the whole range of the Lévy index  $\alpha$ . In Ref. [51] the analysis was restricted to the region  $1 < \alpha < 2$ , at the same time the numerical analysis of the Langevin equation is complemented by numerical solution of space-fractional Fokker-Planck equation.

The main goal of the present paper is to develop analytical theory of the Lévy ratchet and to verify its predictions by numerical simulations. We have found that the probabilistic method of decomposition successfully applied to the escape problem for LFs in Refs. [45,46] also works for the Lévy ratchet description. As potential applications we can mention, following Ref. [51], a ratchet-like transport of impurities in magnetically confined fusion plasmas [57], and a ratchet transport in biology, since biological systems are intrinsically far from equilibrium [58].

The rest of the paper is organized as follows. In Section 2 we formulate the Lévy ratchet model. In Section 3 we give the essentials of the probabilistic decomposition method and present the results of analytical theory. In Section 4 we compare analytical results with the results of numerical simulations. The conclusions and summary are presented in Section 5.

## 2 Model of the Lévy ratchet

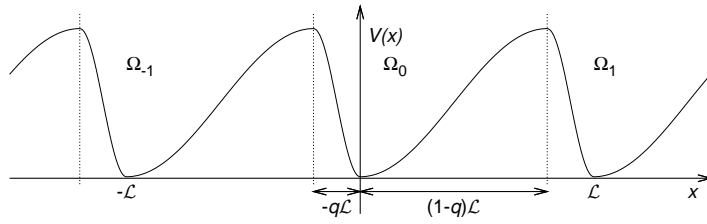


**Fig. 1.** Exemplary potential used for inspection of the ratchet problem. The length of the potential segment is controlled by  $\mathcal{L}$  while the asymmetry of the potential is controlled by the potential asymmetry parameter  $q$  ( $0 < q < 1$ ). For  $q = 1/2$  the potential is symmetric.

We study the following Langevin equation for an overdamped particle driven by the Lévy stable noise  $\dot{L} = dL/dt$

$$\dot{x}(t) = -V'(x) + \varepsilon \dot{L}(t), \quad (1)$$

where  $V(x)$  is the potential, the prime denotes spatial derivative, and  $\varepsilon$  is the amplitude of the noise, which will be considered to be small. The potential  $V(x)$  is periodic,  $V(x) = V(x + \mathcal{L})$ , with potential wells  $\Omega_j$ ,  $j = 0, \pm 1, \pm 2, \dots$ . The  $j$ -th potential well  $\Omega_j$  is located at  $x \in (-\mathcal{L}q + j\mathcal{L}, \mathcal{L}(1-q) + j\mathcal{L})$  where  $0 < q < 1$ , see Fig. 1. As an exemplary potential  $V(x)$  we use

$$V(x) = \begin{cases} V_0 \left[ 1 - \cos \frac{\pi x}{a_1} \right], & 0 \leq x < a_1, \\ V_0 \left[ 1 + \cos \frac{\pi(x-a_1)}{a_2} \right], & a_1 \leq x < \mathcal{L}, \end{cases} \quad (2)$$

where  $\mathcal{L} = a_1 + a_2$ ,  $a_1 = (1-q)\mathcal{L}$  and  $a_2 = q\mathcal{L}$ . The potential lacks reflection symmetry when  $q \neq 1/2$ . Compared with the  $V_0 [\sin(2\pi x/\mathcal{L}) + \sin(4\pi x/\mathcal{L})/4]$  potential typically used in literature, e.g. [55], Eq. (2) offers an advantage of an easier control of the spatial asymmetry. In all the calculations presented below we use  $V_0 = \mathcal{L} = 1$ . Figure 1 presents exemplary potential profile given by Eq. (2).

In the integral form, Eq. (1) reads

$$x(t) = x(0) - \int_0^t V'(x(s)) ds + \varepsilon L(t), \quad (3)$$

where  $L(t)$  is the Lévy stable motion, that is the (formal) integral over the Lévy stable noise in time. For  $\alpha \neq 1$ , the Fourier-transform of  $L(t)$ , see Eqs. (1) and (3), is

$$\langle e^{ikL(t)} \rangle = \exp \left[ -tc|k|^\alpha \left( 1 - i\beta \operatorname{sgn} k \tan \frac{\pi\alpha}{2} \right) \right], \quad (4)$$

where  $\alpha \in (0, 2]$  is the stability index,  $\beta \in [-1, 1]$  is the asymmetry (skewness) parameter, while  $c$  is a positive constant,  $c^{1/\alpha}$  being called a scale parameter. Initially, a particle starts its motion in the minimum of the potential, e.g. in the 0-th potential well. Furthermore, we assume  $\beta \neq \pm 1$ .

### 3 Analytical approach to the Lévy ratchet

Analytical approach to the transport in a ratchet potential under action of Lévy noise is based on the decomposition method, for which the main results were presented in [45], whereas the mathematical details including proofs of corresponding theorems were given in [46]. Then, the dynamics in multi-well potentials was considered in [47]. Our exposition of the Lévy ratchet is based essentially on these three papers. In Section 3 we first give an “intuitive” explanation of the decomposition method and then present theoretical results for main characteristics of ratchet transport, namely the mean exit time from a single well, a transition probability, a mean displacement and the current.

#### 3.1 Method of decomposition and single-well dynamics in case of symmetric Lévy noise

Let us consider the discretized version of Eq. (1) with the time step of integration  $\Delta t$ ,

$$x(n+1) - x(n) = -V'(x(n))\Delta t + \xi(n), \quad (5)$$

where  $\xi(n) = L(n\Delta t) - L((n-1)\Delta t) = \varepsilon(c\Delta t)^{1/\alpha}\zeta(n)$  is the value of the noise variable, or the Lévy jump, at the  $n$ -th interval of integration. Here,  $\zeta(n)$  is the time-discrete Lévy noise whose characteristic function is given by Eq. (4) with  $t = 1$ ,  $c = 1$ . Thus, the PDF of these Lévy jumps  $p = p(\xi)$  is characterized by the scale parameter, or characteristic length  $w = \varepsilon(c\Delta t)^{1/\alpha}$  depending on the parameters of the noise and on the length  $\Delta t$  of the time interval.

For the further exposition it is necessary to recall the asymptotics of the tails of the PDF  $p(\xi)$  as  $\xi \rightarrow \pm\infty$  given e.g. in [59, Chapter 4.3]:

$$p(\xi) \simeq c\Delta t\varepsilon^\alpha \frac{1 \pm \beta}{2 \cos(\frac{\alpha\pi}{2})|\Gamma(-\alpha)|} \frac{1}{\xi^{1+\alpha}} = A_\pm w^\alpha \frac{1}{|\xi|^{1+\alpha}}, \quad \xi \rightarrow \pm\infty, \quad |\xi| \gg w \quad (6)$$

Let us fix some level  $\delta > 0$  (depending on  $\varepsilon$ ) and decompose the noise  $\xi(n)$  into two parts: Thus all  $\xi(n)$  smaller in absolute value than  $\delta$  are considered to belong to the background part of the noise (containing most of  $\xi(n)$ ), and large spikes with  $|\xi(n)| > \delta$  form a shot-like noise containing rare events, or outliers, see Fig. 2 showing the decomposition schematically. Since the values  $\xi(n)$  are independent, the probability that a spike occurs on the step  $n$  does not depend on  $n$  and equals to  $P_{\text{spike}} = \int_{-\infty}^{-\delta} p(\xi)d\xi + \int_{\delta}^{\infty} p(\xi)d\xi$ . For  $\varepsilon$  and  $\Delta t$  small enough the characteristic length  $w$  is small, thus the probability  $P_{\text{spike}}$  is determined by the large argument asymptotics of the Lévy stable density given by Eq. (6),  $p(\xi) \simeq A_\pm w^\alpha |\xi|^{-(1+\alpha)}$ ,  $\xi \rightarrow \pm\infty$ , and behaves as  $P_{\text{spike}} \simeq (A/\alpha)c\Delta t\varepsilon^\alpha\delta^{-\alpha}$ , where  $A = A_- + A_+$ . Therefore, the spikes form a Poissonian sequence of events, and, for  $\delta$  large enough, the spikes are well separated in time. The probability to have at least one spike on the unit time interval is

$$P = \frac{Ac}{\alpha}\varepsilon^\alpha\delta^{-\alpha}. \quad (7)$$

The probability not to have a spike on a time interval  $[0, t]$  is around  $(1 - (Ac/\alpha)\varepsilon^\alpha\delta^{-\alpha}\Delta t)^{t/\Delta t} \simeq \exp(-t/T)$  with

$$T = \frac{\alpha}{Ac}\varepsilon^{-\alpha}\delta^\alpha \quad (8)$$

being the mean time between two subsequent spikes. On the other hand, the background part of the noise has finite variance  $\sigma^2$  and its action over time intervals much larger than  $\Delta t$  can be

modelled by the action of a white Gaussian noise. The variance of the background component is given by  $\sigma^2 = \text{var}(\xi(n) | |\xi(n)| \leq \delta)$  and, for large enough  $\delta$ , is again determined by the power-law asymptotics of the Lévy stable density in its far tail:  $\sigma^2 \simeq \text{const} \times \varepsilon^\alpha \delta^{2-\alpha} \Delta t$ . The variance introduced by the background noise over the unit time interval (the background noise strength) due to the role of summation of variances for the white noise behaves as

$$\sigma^2 \simeq \text{const} \times \varepsilon^\alpha \delta^{2-\alpha}. \quad (9)$$

For  $\varepsilon \rightarrow 0$  it is always possible to choose  $\delta$  in such a way that both  $P$  in Eq. (7) and  $\sigma^2$  in Eq. (9) tend to zero. In Refs. [45,46] the value of  $\delta = \varepsilon^{1/2}$  was taken effectively to obtain the necessary estimates.

Let us now fix small  $\varepsilon$  and take  $\delta$  as discussed above. Between the two subsequent large spikes the particle is subjected only to a background noise, which, for small  $\varepsilon$ , is so weak that the motion of a particle is almost deterministic, namely the particle slides towards the bottom of the potential well. The overall structure of such motion is well seen in the bottom panel of Fig. 2. For  $\varepsilon$  small enough the background noise can be neglected, which would correspond to smoothing the rugged curve in the bottom panel of the figure and approximating it by a deterministic trajectory. On the other hand, the time lag between the two subsequent spikes is so large that the particle reaches the bottom of the potential well between the two spikes. The only process of escape possible in this case, corresponds to the possibility that a strong enough spike “kicks” the particle from the bottom of the potential well, and an escape occurs in a single jump if its length exceeds the distance between the potential’s minimum and maximum, see Fig. 2. The probability of jumping out of the well  $\Omega_0$  is the conditional probability of having a positive spike larger than  $(1-q)\mathcal{L}$  or having a negative spike larger than  $q\mathcal{L}$  in absolute value, that is

$$P_{\text{exit}} \simeq \text{Prob}\left\{\xi(n) < -q\mathcal{L} \text{ or } \xi(n) > (1-q)\mathcal{L} \mid |\xi(n)| > \delta\right\} = \frac{\int_{-\infty}^{-q\mathcal{L}} p(\xi) d\xi + \int_{(1-q)\mathcal{L}}^{\infty} p(\xi) d\xi}{\int_{-\infty}^{-\delta} p(\xi) d\xi + \int_{\delta}^{\infty} p(\xi) d\xi}, \quad (10)$$

where the wings of the Lévy stable PDF representing the action of spikes per unit time are given by  $p(\xi) \simeq A_{\pm} w^\alpha \xi^{-1-\alpha}$ ,  $\xi \rightarrow \pm\infty$ . Thus, we get

$$P_{\text{exit}} \simeq \left(\frac{A_-}{q^\alpha} + \frac{A_+}{(1-q)^\alpha}\right) \frac{\delta^\alpha}{A\mathcal{L}^\alpha}, \quad (11)$$

which reproduces the result of Ref. [47].

Now we are able to calculate the mean exit time from a single well. Indeed, exit on a  $k$ -th spike means that the first  $(k-1)$  attempts were unsuccessful, and the  $k$ -th jump was big enough. The probability of this event approximately equals  $(1 - P_{\text{exit}})^{k-1} P_{\text{exit}}$ . The mean exit time in this case equals  $kT$  where the mean interspike time  $T$  is known, see Eq. (8). This yields

$$\begin{aligned} \langle \tau(\varepsilon) \rangle &\simeq \sum_{k=1}^{\infty} kT(1 - P_{\text{exit}})^{k-1} P_{\text{exit}} = \frac{T}{P_{\text{exit}}} \\ &= \left[ \frac{c}{2\alpha \cos \frac{\pi\alpha}{2} |\Gamma(-\alpha)|} \left( \frac{1+\beta}{(1-q)^{-\alpha}} + \frac{1-\beta}{q^{-\alpha}} \right) \right]^{-1} \times \frac{\mathcal{L}^\alpha}{\varepsilon^\alpha}. \end{aligned} \quad (12)$$

The picture of escape at small  $\varepsilon$  differs drastically from the Kramers picture, namely instead of climbing up in the potential well the particle is thrown out from the well by a single large kick. Due to the fact that potential is translationally invariant the mean exit times  $\langle \tau^i(\varepsilon) \rangle$  for all the potential wells are the same and equal to  $\langle \tau(\varepsilon) \rangle$ .

Now we can derive the asymptotic value of the transition probability  $p_{i,i+k}$  for a particle to make a jump from the  $i$ -th potential well to the  $(i+k)$ -th well. Assume for brevity that the particle starts at the well  $\Omega_0$ ,  $i = 0$ , and jumps to the well  $\Omega_k$ ,  $k \geq 1$ . The probability  $p_k = p_{0,k}$  is then obtained similarly to Eq. (12). Indeed, the transition to the well  $\Omega_k$  occurs if

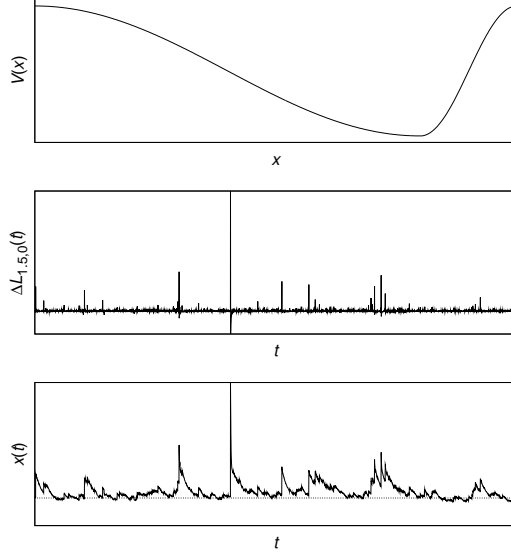


**Fig. 2.** Sample realization of the escape problem (bottom panel) driven by the Lévy noise with parameters  $\alpha = 1.1$  and  $\beta = 0.9$  (middle panel). A particle moves in a potential well  $\Omega_0$  (top panel).

the kick  $\xi(n)$  overcomes the distance  $(1 - q)\mathcal{L} + (k - 1)\mathcal{L}$  but is smaller than  $(1 - q)\mathcal{L} + k\mathcal{L}$ . The probability of this event equals to

$$P_{0 \rightarrow k} \simeq \text{Prob}\left\{\xi(n) \in [(k - q)\mathcal{L}, (k + 1 - q)\mathcal{L}] \mid |\xi(n)| > \delta\right\} = \frac{\int_{(k-q)\mathcal{L}}^{(k+1-q)\mathcal{L}} p(\xi) d\xi}{\int_{-\infty}^{-\delta} p(\xi) d\xi + \int_{\delta}^{\infty} p(\xi) d\xi} \quad (13)$$

$$= \left(\frac{1}{(k - q)^\alpha} - \frac{1}{(k + 1 - q)^\alpha}\right) \frac{A_+}{A} \frac{\delta^\alpha}{\mathcal{L}^\alpha}.$$

Then with the help of the formula of the total probability we get

$$p_{i,i+k} = p_k \simeq \sum_{k=1}^{\infty} (1 - P_{\text{exit}})^{k-1} P_{0 \rightarrow k} = \frac{P_{0 \rightarrow k}}{P_{\text{exit}}} = (1 + \beta) \frac{(k - q)^{-\alpha} - (k + 1 - q)^{-\alpha}}{(1 - \beta)q^{-\alpha} + (1 + \beta)(1 - q)^{-\alpha}}. \quad (14)$$

Analogously, considering negative jumps we calculate transition probabilities  $p_k = p_{i,i+k}$  for  $k \leq -1$  as

$$p_{i,i+k} = p_k \simeq (1 - \beta) \frac{(-k - 1 + q)^{-\alpha} - (-k + q)^{-\alpha}}{(1 - \beta)q^{-\alpha} + (1 + \beta)(1 - q)^{-\alpha}}. \quad (15)$$

### 3.2 Characteristics of transport

A particle inserted into the  $i$ -th potential well spends a random time within the potential well, until it is kicked out of the well by a large spike, as it is described in subsection 3.1. It can be shown that in the small noise limit  $\varepsilon \rightarrow 0$ , the first exit time  $\tau^i(\varepsilon)$  from  $i$ -th potential  $\Omega_i$  is an exponentially distributed random variable with the mean value  $\langle \tau^i(\varepsilon) \rangle = \langle \tau(\varepsilon) \rangle$ , see Eq. (12). The transition probability  $p_{i,i+k}$  for a particle to make a jump from the  $i$ -th potential well to the  $(i + k)$ -th potential well is given by Eqs. (14) and (15).

### 3.2.1 Splitting probabilities

In order to elucidate the asymmetry of the first escape we use the splitting probability  $\pi$  which is a probability of a first escape from a potential well to the right

$$\pi_R(\alpha, \beta, q) = \sum_{k \geq 1} p_k = \frac{(1 + \beta)(1 - q)^{-\alpha}}{(1 - \beta)q^{-\alpha} + (1 + \beta)(1 - q)^{-\alpha}}, \quad (16)$$

or to the left

$$\pi_L(\alpha, \beta, q) = \sum_{k \leq -1} p_k = \frac{(1 - \beta)q^{-\alpha}}{(1 - \beta)q^{-\alpha} + (1 + \beta)(1 - q)^{-\alpha}}. \quad (17)$$

Due to the asymmetry of the noise it is possible to find such a set of parameters for which the two values of splitting probabilities are equal. The balance condition

$$\pi_L(\alpha, \beta, q) = \pi_R(\alpha, \beta, q) = \frac{1}{2} \quad (18)$$

leads to the skewness parameter

$$\beta_\pi(\alpha, q) = \frac{(1 - q)^\alpha - q^\alpha}{(1 - q)^\alpha + q^\alpha}. \quad (19)$$

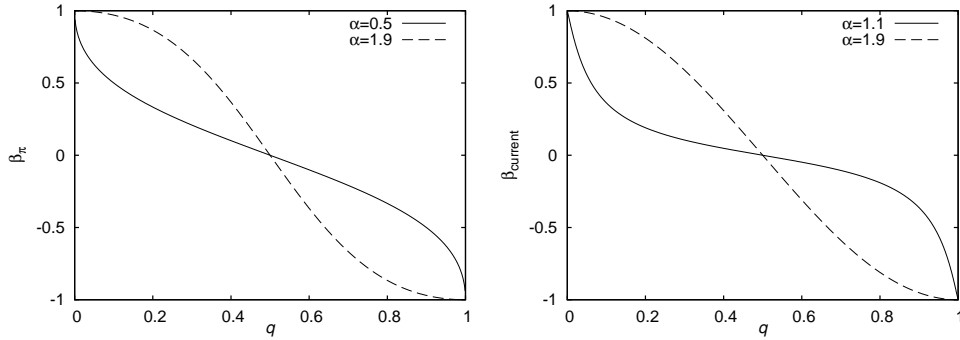


**Fig. 3.** The left panel presents values of the noise asymmetry  $\beta_\pi$  leading to equal values of splitting probabilities, see Eq. (19). The right panel presents values of the noise asymmetry  $\beta_{\text{current}}$  leading to zero current, see Eq. (24).

### 3.2.2 Mean displacement

For  $\alpha > 1$ , the mean displacement of the particle at the time  $t$  is

$$\langle X^\varepsilon(t) \rangle = \langle n \rangle \Lambda, \quad (20)$$

where  $\langle n \rangle = t / \langle \tau(\varepsilon) \rangle$  is the average number of jumps during time  $t$ . The mean value of the displacement  $\Lambda$  can be expressed as

$$\Lambda = \mathcal{L} \sum_{k=-\infty, k \neq 0}^{\infty} k p_k = W_+(\alpha, \beta, q) - W_-(\alpha, \beta, q), \quad (21)$$

where

$$W_+(\alpha, \beta, q) = \mathcal{L} \sum_{k \geq 1} k p_k = \mathcal{L} \frac{(1 + \beta) \zeta(\alpha, 1 - q)}{(1 - \beta) q^{-\alpha} + (1 + \beta)(1 - q)^{-\alpha}}$$

and

$$W_-(\alpha, \beta, q) = -\mathcal{L} \sum_{k \leq -1} k p_k = \mathcal{L} \frac{(1 - \beta) \zeta(\alpha, q)}{(1 - \beta) q^{-\alpha} + (1 + \beta)(1 - q)^{-\alpha}}.$$

In above equations  $\zeta(\alpha, q)$  denotes the Hurwitz zeta function,  $\zeta(\alpha, q) = \sum_{k=0}^{\infty} (k + q)^{-\alpha}$ . The mean jump length  $\Lambda$ , see Eq. (20), and consequently the mean displacement  $\langle X^\varepsilon(t) \rangle$ , see Eq. (21), are finite for  $\alpha > 1$  only.

The main characteristics of the particles' transport in the Lévy ratchet is the particle current. For the stability index  $\alpha > 1$ , the current is defined as the time derivative of  $\langle X^\varepsilon(t) \rangle$ ,

$$j(\alpha, \beta, q) = \frac{d}{dt} \langle X^\varepsilon(t) \rangle = \frac{W_+(\alpha, \beta, q) - W_-(\alpha, \beta, q)}{\langle \tau(\varepsilon) \rangle}.$$

Consequently, for small noise intensities  $\varepsilon \rightarrow 0$  we get

$$j(\alpha, \beta, q) \propto \varepsilon^\alpha. \quad (22)$$

The multiplicative constant in Eq. (22) depends on parameters  $\alpha$  and  $\beta$  of the noise and on the asymmetry parameter  $q$  of the potential.

We also determine the skewness parameter  $\beta$  of the noise, which leads to the zero particles' current. Indeed, the balance equation

$$j(\alpha, \beta, q) = 0 \quad (23)$$

yields the unique solution

$$\beta_{\text{current}}(\alpha, q) = \frac{\zeta(\alpha, q) - \zeta(\alpha, 1 - q)}{\zeta(\alpha, q) + \zeta(\alpha, 1 - q)}. \quad (24)$$

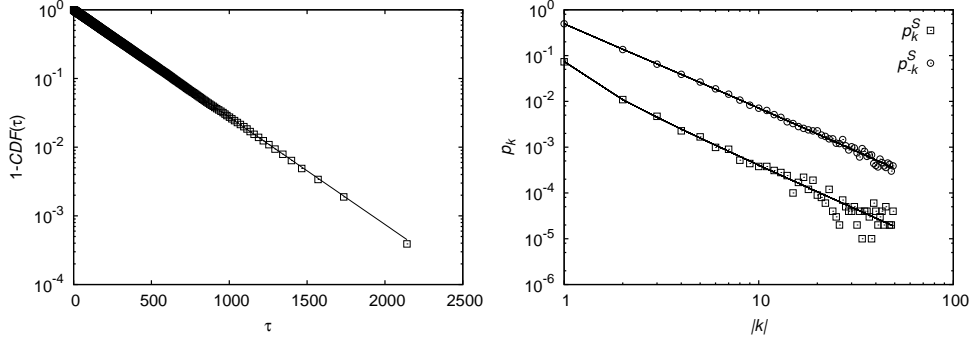
## 4 Numerical validation of the theory

In order to show validity of the developed theory extensive numerical simulations have been performed for the stability index  $\alpha \in \{0.7, 0.9, 1.1, 1.5, 1.9\}$ , the noise asymmetry parameter  $\beta \in \{0.0, \pm 0.5, \pm 0.9\}$  and the potential asymmetry parameter  $q \in \{0.2, 0.3, 0.4, 0.5, 0.6, 0.7, 0.8\}$  with various (decreasing) noise intensities  $\varepsilon$ . Numerical results were constructed by standard methods of integration of stochastic differential equations with respect to  $\alpha$ -stable noises, see Refs. [60,61,62,63]. All numerical simulations have been performed with the time step of integration  $\Delta t = 10^{-3}$ , the number of realizations  $N = 10^5$ , the potential depth  $V_0 = 1$ , the scale parameter  $c = 1$  and the potential segment length  $\mathcal{L} = 1$ . In general, all simulations in the limit of weak noise (small  $\varepsilon$ ) converge to theoretical predictions. From the whole set of simulations we have chosen exemplary results presented in Figs. 4–11.

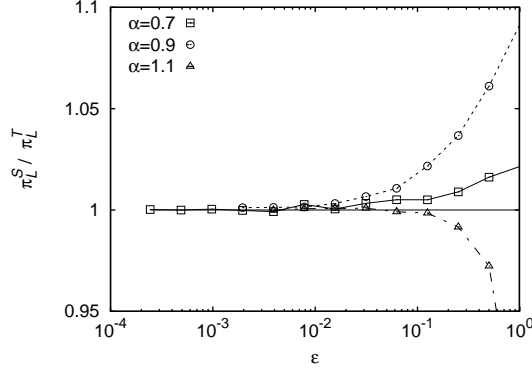
Figure 4 presents the complementary cumulative distribution of the exit time  $1 - CDF(\tau)$  (left panel) and the transition probabilities  $p_k$  (right panel) for the stability index  $\alpha = 0.9$ , the noise asymmetry  $\beta = -0.9$  and the potential asymmetry  $q = 0.7$ . The left panel of Fig. 4 demonstrates the exponential character of the exit time distribution whereas the right panel of Fig. 4 compares theoretical transition probabilities from the initial potential well  $\Omega_0$  to the well  $\Omega_k$  given by Eqs. (14) and (15) (solid lines) with their numerical estimators (symbols), demonstrating perfect agreement between theoretical predictions and numerical simulations.

Fig. 5 demonstrates the ratio of the numerically estimated values of the splitting probabilities  $\pi_L^S$  and their theoretical values  $\pi_L^T$  given by Eq. (17) for different values of  $\alpha$ . In the limit





**Fig. 4.** The left panel demonstrates the exponential character of the (first) exit time distribution. The solid line in the left panel presents  $\exp[-\tau/\langle\tau\rangle^T]$ . The right panel presents transition probabilities  $p_k$  from the initial potential well (0) to the final potential well ( $k$ ). Circles and squares represent simulation results, while thin solid lines correspond to analytical formulas given by Eqs. (14) and (15). Simulation parameters: the stability index  $\alpha = 0.9$ , the noise asymmetry  $\beta = -0.9$ , the potential asymmetry  $q = 0.7$  and the noise intensity  $\varepsilon = 2^{-9}$ .



**Fig. 5.** Ratio of simulated and theoretical values of splitting probabilities  $\pi_L^S/\pi_L^T$ . Simulation parameters: the noise asymmetry  $\beta = -0.9$ , the potential asymmetry  $q = 0.7$ .

of the small noise intensity the ratio between estimated and theoretical values of splitting probabilities tends to 1 indicating the agreement between the theory and simulations. For larger noise intensities numerical results deviate from predictions for weak noise regime. The sign of this deviation is different for  $\alpha > 1$  and for  $\alpha < 1$ .

The left panel of Fig. 6 displays the ratio between the numerically estimated mean exit time  $\langle\tau(\varepsilon)\rangle^S$  and the theoretical prediction  $\langle\tau(\varepsilon)\rangle^T$ , see Eq. (12). In the limit of small noise intensities  $\varepsilon$  the ratio between estimated and theoretical values of mean exit times tends to 1 indicating that simulations performed corroborate theoretical findings. The right panel of Fig. 6 shows the scaling of the estimated mean exit time  $\langle\tau(\varepsilon)\rangle$  (symbols) with the noise intensity  $\varepsilon$  along with the corresponding theoretical prediction, see Eq. (12), shown as solid lines. Deviations from the predicted scaling visible for large noise intensities vanish for small values of  $\varepsilon$ .

Fig. 7 displays the splitting probability  $\pi_R$  given by Eq. (16) as a function of potential asymmetry  $q$  for the case of symmetric Lévy noise with  $\beta = 0$  and different  $\alpha$ . Here again the close agreement between analytical formulas and numerical results is observed. For symmetric noise and symmetric potential ( $q = 0.5$ ) splitting probability is equal to 0.5. This indicates absence of the current in the system at hand.

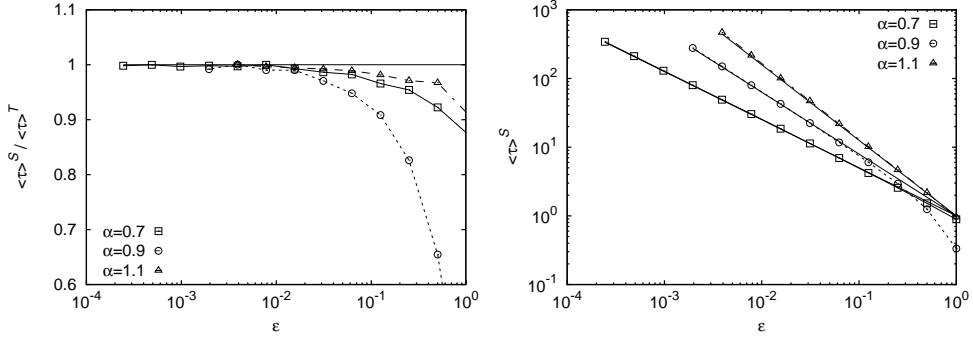


**Fig. 6.** The left panel demonstrates the ratio of simulated and theoretical values of the mean escape time  $\langle\tau\rangle^S / \langle\tau\rangle^T$ . The right panel presents the power-law scaling of the mean escape time as a function of the noise intensity  $\varepsilon$ . Points represent simulation results while solid lines indicate the theoretical scaling of the mean exit time  $\langle\tau\rangle$  with the noise intensity  $\varepsilon$ . Simulation parameters: the noise asymmetry  $\beta = -0.9$ , the potential asymmetry  $q = 0.7$ .

The left panel of Fig. 8 presents the mean displacement  $\Lambda$  defined for  $\alpha > 1$  only and given by Eq. (21), and its numerical value estimated as

$$\Lambda^S = \langle\Lambda_i\rangle, \quad (25)$$

$\Lambda_i$  being the number of the potential well to which a random walker was thrown from the initial one. For all values of  $\alpha$  except for  $\alpha = 1.1$ , which is too close to the boundary of convergence, the agreement between the numerical and the theoretical values is good. The right panel of Fig. 8 presents the splitting probability  $\pi_R$  as a function of the potential asymmetry  $q$  for the case of asymmetric Lévy noise with  $\beta = 0.9$ . The numerical values (symbols) agree well with theoretical predictions (lines).

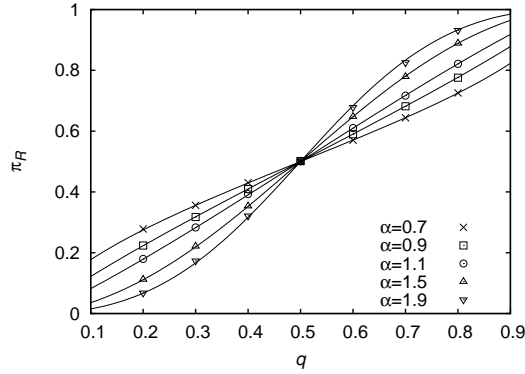


**Fig. 7.** Theoretical (solid lines) and simulated (points) values of the splitting probability  $\pi_R$  as a function of the potential asymmetry  $q$ . Various curves correspond to different values of the stability index  $\alpha$ . Simulation parameters: the noise asymmetry  $\beta = 0.0$ , the noise intensity  $\varepsilon = 2^{-9}$  and the potential asymmetry  $q = 0.7$ .

Fig. 9 demonstrates the value of the splitting probability  $\pi_L$  observed for the value of  $\beta_\pi$  given by Eq. (19) (left panel) and values of the noise asymmetry parameter  $\beta_\pi$  leading to equal values of splitting probabilities, see Eq. (19), (right panel). Results presented in Fig. 9 correspond to  $\varepsilon = 2^{-6}$ , which is larger than  $\varepsilon$  in remaining figures. This is due to the fact that for noise asymmetry  $\beta_\pi$  given by Eq. (19) longer simulation time is necessary.

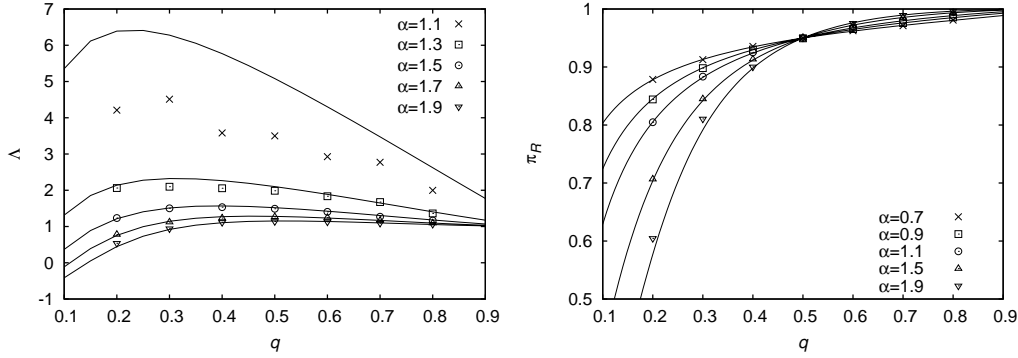


**Fig. 8.** Theoretical (solid lines) and simulated (points) values of the mean displacement  $\Lambda^S = \langle \Lambda_i \rangle$  (left panel) and theoretical (solid lines) and simulated (points) values of the splitting probability  $\pi_R$  (right panel). Simulation parameters: the noise asymmetry  $\beta = 0.9$ , the noise intensity  $\varepsilon = 2^{-9}$  and the potential asymmetry  $q = 0.7$ .

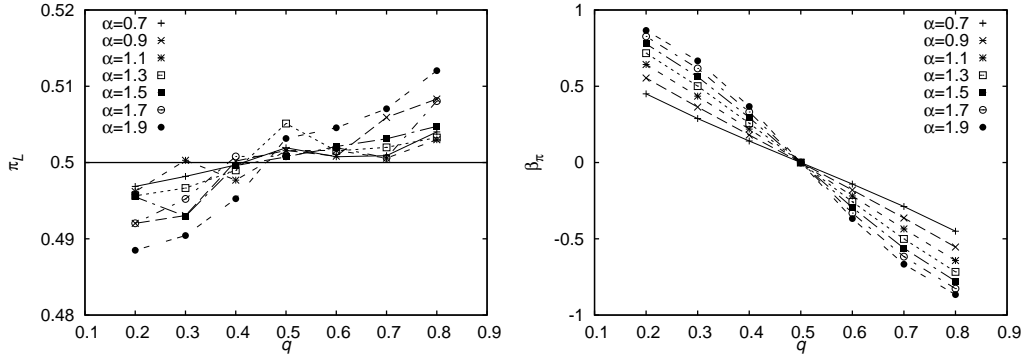


**Fig. 9.** The left panel presents the simulated splitting probability  $\pi_L$  for the set of parameters for which the balance equality  $\pi_L = \pi_R = 0.5$  should hold. The right panel presents values of the noise asymmetry  $\beta_\pi$  leading to equal values of splitting probabilities, see Eq. (19). Simulation parameters:  $\varepsilon = 2^{-6}$ .

The left panels of Figs. 10 and 11 compare theoretical values of the current given by Eq. (22) with their numerical estimates as functions of the noise intensity  $\varepsilon$  at time  $t = 2000$ . The power-law dependence  $j \propto \varepsilon^\alpha$  of the current, see Eq. (22) is clearly demonstrated. For symmetric noises, see Fig. 10, the absolute values of the current for  $q = 0.3$  and  $q = 0.7$  are the same. For  $q = 0.5$ , the theoretical value of the current vanishes, while numerical results fluctuate at a very low level. The right panels of Figs. 10 and 11 present the dependence of the current  $j$  on time  $t$  for symmetric ( $\beta = 0$ ) and asymmetric ( $\beta = 0.9$ ) noise, respectively. Various curves correspond to different values of the potential asymmetry  $q$ . After a short transient the current reaches a constant value corresponding to a stationary regime of operation.

## 5 Summary

In this paper we have considered the transport properties of a particle embedded in a ratchet potential and subjected to a white Lévy noise. In the case of weak noise the decomposition method proposed in Refs. [45,46] allowed us to calculate such characteristics of this transport as splitting probabilities of the first escape from a single well of a ratchet potential, the transition probability, the mean displacement of a particle and the particle current. In order

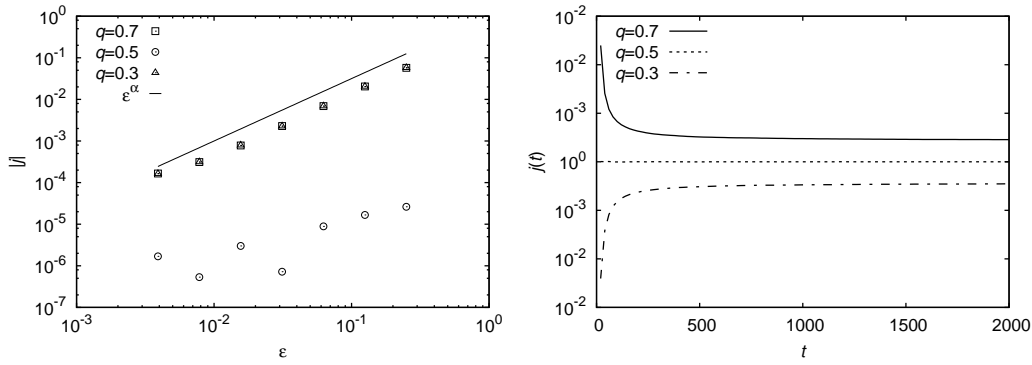


**Fig. 10.** The left panel presents the current  $j$  as a function of the noise intensity  $\varepsilon$  at  $t = 2000$  and various values of the potential asymmetry. The solid line presents theoretical scaling of the current on  $\varepsilon$ . The right panel represents the current  $j$  as a function of time for the symmetric Lévy noise and various values of potential asymmetry  $q$ . Simulation parameters:  $\alpha = 1.5$ ,  $\beta = 0$ , and  $\varepsilon = 2^{-5}$ .

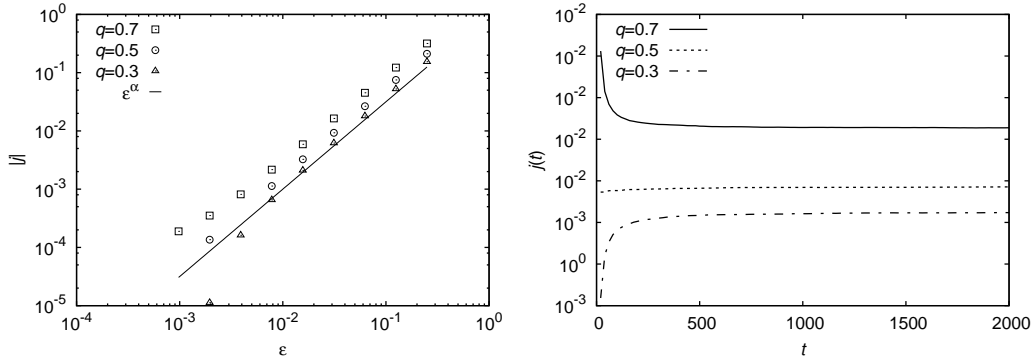


**Fig. 11.** The same as in Fig. 10 for asymmetric Lévy noise with  $\beta = 0.9$ . Simulation parameters:  $\alpha = 1.5$ ,  $\varepsilon = 2^{-6}$ .

to confirm analytical results, we performed an extensive numerical simulations demonstrating good agreement with the theory at small values of the noise intensity.

The authors acknowledge support by DFG within SFB555. AVC acknowledges financial support from European Commission via MC IIF, grant 219966 LeFrac. Computer simulations have been performed at Institute of Physics, Jagellonian University and Academic Computer Center, Cyfronet AGH.

## References

1. P. P. Lévy. *Théorie de l'addition des variables aléatoires*. Gauthier-Villars, Paris, 1937.
2. B. Mandelbrot. *The Fractal Geometry of Nature*. W. H. Freeman, New York, 1983.
3. W. Feller. *An introduction to probability theory and its applications: volume II*. John Wiley & Sons, 1971.
4. B. V. Gnedenko and A. N. Kolmogorov. *Limit distributions for sums of independent random variables*. Addison-Wesley Publishing Company, Cambridge, Mass., 1954.
5. G. Samorodnitsky and M. S. Taqqu. *Stable non-Gaussian random processes*. Chapman&Hall/CRC, 1994.
6. M. F. Shlesinger, G. M. Zaslavsky, and J. Klafter. Strange kinetics. *Nature*, 363(6424):31–37, 1993.
7. J. Klafter, M. F. Shlesinger, and G. Zumofen. Beyond Brownian motion. *Physics Today*, 49(2):33, 1996.

8. T. H. Solomon, E. R. Weeks, and H. L. Swinney. Observation of anomalous diffusion and Lévy flights in a two-dimensional rotating flow. *Physical Review Letters*, 71(24):3975—3978, 1993.
9. D. del Castillo-Negrete. Asymmetric transport and non-Gaussian statistics of passive scalars in vortices in shear. *Physics of Fluids*, 10(3):576–594, 1998.
10. A. V. Chechkin, V. Yu. Gonchar, and M. Szydlowski. Fractional kinetics for relaxation and superdiffusion in a magnetic field. *Physics of Plasmas*, 9(1):78–88, 2002.
11. V. Yu. Gonchar, A. V. Chechkin, E. L. Sorokovoi, V. V. Chechkin, and E. D. Volkov. Stable Lévy distributions of the density and potential fluctuations in the edge plasma of the *U-3M* torsatron. *Plasma Physics Reports*, 29(5):380–390, 2003.
12. T. Mizuuchi, V. V. Chechkin, K. Ohashi, E. L. Sorokovoy, A. V. Chechkin, V. Yu. Gonchar, K. Takahashi, S. Kobayashi, H. Okada K. Nagasaki, S. Yamamoto, F. Sano, K. Kondo, N. Nishino, H. Kawazome, H. Shidara, S. Kaneko, Y. Fukagawa, Y. Morita, S. Nakazawa, S. Nishio, S. Tsuboi, and M. Yamada. Edge fluctuation studies in Heliotron J. *Journal of Nuclear Materials*, 337–339:332–336, 2005.
13. D. del Castillo-Negrete, B. A. Carreras, and V. E. Lynch. Nondiffusive transport in plasma turbulence: A fractional diffusion approach. *Physical Review Letters*, 94(6):065003, 2005.
14. H. Katori, S. Schlipf, and H. Walther. Anomalous dynamics of a single ion in an optical lattice. *Physical Review Letters*, 79(12):2221–2224, 1997.
15. A. Carati, L. Galgani, and B. Pozzi. Lévy flights in the Landau-Teller model of molecular collisions. *Physical Review Letters*, 90(1):010601, 2003.
16. C.-K. Peng, J. Mietus, J. M. Hausdorff, S. Havlin, H. E. Stanley, and A. L. Goldberger. Long-range anticorrelations and non-Gaussian behavior of the heartbeat. *Physical Review Letters*, 70(9):1343–1346, 1993.
17. R. Segev, M. Benveniste, E. Hulata, N. Cohen, A. Palevski, E. Kapon, Y. Shapira, and E. Ben-Jacob. Long term behavior of lithographically prepared *in vitro* neuronal networks. *Physical Review Letters*, 88(11):118102, 2002.
18. M. A. Lomholt, T. Ambjörnsson, and R. Metzler. Optimal target search on a fast folding polymer chain with volume exchange. *Physical Review Letters*, 95(26):260603, 2005.
19. G. M. Viswanathan, V. Afanasyev, S. V. Buldyrev, E. J. Murphey, P. A. Prince, and H. E. Stanley. Lévy flight search patterns of wandering albatrosses. *Nature*, 381:413–415, 1996.
20. O. Sotolongo-Costa, J. C. Antoranz, A. Posadas, F. Vidal, and A. Vázquez. Lévy flights and earthquakes. *Geophysical Research Letters*, 27(13):1965–1968, 2000.
21. P. D. Ditlevsen. Observation of  $\alpha$ -stable noise induced millennial climate changes from an ice record. *Geophysical Research Letters*, 26(10):1441–1444, May 1999.
22. S. A. Kassam. *Signal Detection in Non-Gaussian Noise*. Springer Texts in Electrical Engineering. Springer, 1988.
23. E. J. Wegman, J. B. Thomas, and S. C. Schwartz, editors. *Topics in Non-Gaussian Signal Processing*. Springer-Verlag, 1988.
24. C. L. Nikias and M. Shao. *Signal processing with alpha-stable distributions and applications*. Wiley-Interscience, New York, NY, USA, 1995.
25. R. N. Mantegna and H. E. Stanley. *An Introduction to Econophysics: Correlations and Complexity in Finance*. Cambridge University Press, 1999.
26. J.-P. Bouchaud and M. Potters. *Theory of Financial Risks: From Statistical Physics to Risk Management*. Cambridge University Press, 2000.
27. R. E. Gomory and B. B. Mandelbrot. *Fractals and Scaling In Finance: Discontinuity, Concentration, Risk*. Springer, 1997.
28. D. Brockmann, L. Hufnagel, and T. Geisel. The scaling laws of human travel. *Nature*, 439:462–465, 2006.
29. P. Barthelemy, J. Bertolotti, and D. S. Wiersma. A Lévy flight for light. *Nature*, 453:495–498, 2008.
30. N. Mercadier, W. Guerin, M. Chevrollier, and R. Kaiser. Lévy flights of photons in hot atomic vapours. *Nature Physics*, 5:602–605, 2009.
31. S. Jespersen, R. Metzler, and H. C. Fogedby. Lévy flights in external force fields: Langevin and fractional Fokker-Planck equations and their solutions. *Physical Review E*, 59(3):2736–2745, 1999.
32. A. V. Chechkin and V. Yu. Gonchar. Linear relaxation processes governed by fractional symmetric kinetic equations. *Journal of Experimental and Theoretical Physics*, 91(3):635–651, 2000.
33. A. V. Chechkin, V. Yu. Gonchar, J. Klafter, R. Metzler, and L. V. Tanatarov. Stationary states of non-linear oscillators driven by Lévy noise. *Chemical Physics*, 284(1-2):233–251, 2002.

34. G. Samorodnitsky and M. Grigoriu. Tails of solutions of certain nonlinear stochastic differential equations driven by heavy tailed Lévy motions. *Stochastic Processes and their Applications*, 105(1):69–97, 2003.
35. G. Samorodnitsky and M. Grigoriu. Characteristic function for the stationary state of a one-dimensional dynamical system with Lévy noise. *Theoretical and Mathematical Physics*, 150(3):332–346, 2007.
36. A. Dubkov and B. Spagnolo. Langevin approach to Lévy flights in fixed potentials: Exact results for stationary probability distributions. *Acta Physica Polonica B*, 38(5):1745–1758, 2007.
37. A. V. Chechkin, J. Klafter, V. Yu. Gonchar, R. Metzler, and L. V. Tanatarov. Bifurcation, bimodality, and finite variance in confined Lévy flights. *Physical Review E*, 67:010102(R), 2003.
38. A. V. Chechkin, V. Yu. Gonchar, J. Klafter, R. Metzler, and L. V. Tanatarov. Lévy flights in a steep potential well. *Journal of Statistical Physics*, 115(5–6):1505–1535, 2004.
39. O. Ditlevsen. Invalidity of the spectral Fokker–Planck equation for Cauchy noise driven Langevin equation. *Probabilistic Engineering Mechanics*, 19(4):385–392, 2004.
40. B. Dybiec, I. M. Sokolov, and A. V. Chechkin. Stationary states in single-well potentials under symmetric Lévy noises. *Journal of Statistical Mechanics: Theory and Experiment*, P07008, 2010.
41. P. D. Ditlevsen. Anomalous jumping in a double-well potential. *Physical Review E*, 60(1):172–179, 1999.
42. A. V. Chechkin, V. Yu. Gonchar, J. Klafter, and R. Metzler. Barrier crossings of a Lévy flight. *Europhysics Letters*, 72(3):348–354, 2005.
43. A. Chechkin, O. Sliusarenko, R. Metzler, and J. Klafter. Barrier crossing driven by Lévy noise: Universality and the role of noise intensity. *Physical Review E*, 75:041101, 2007.
44. B. Dybiec, E. Gudowska-Nowak, and P. Hänggi. Escape driven by  $\alpha$ -stable white noises. *Physical Review E*, 75(2):021109, 2007.
45. P. Imkeller and I. Pavlyukevich. Lévy flights: transitions and meta-stability. *Journal of Physics A: Mathematical and General*, 39:L237–L246, 2006.
46. P. Imkeller and I. Pavlyukevich. First exit times of SDEs driven by stable Lévy processes. *Stochastic Processes and their Applications*, 116(4):611–642, 2006.
47. P. Imkeller and I. Pavlyukevich. Metastable behaviour of small noise Lévy-driven diffusions. *ESAIM: Probability and Statistics*, 12:412–437, 2008.
48. H. Szu and R. Hartley. Fast simulated annealing. *Physics Letters A*, 122(3,4):157–162, 1987.
49. I. Pavlyukevich. Cooling down Lévy flights. *Journal of Physics A: Mathematical and Theoretical*, 40:12299–12313, 2007.
50. I. Pavlyukevich. Lévy flights, non-local search and simulated annealing. *Journal of Computational Physics*, 226(2):1830–1844, 2007.
51. D. del Castillo-Negrete, V. Yu. Gonchar, and A. V. Chechkin. Fluctuation-driven directed transport in the presence of Lévy flights. *Physica A*, 387(27):6693–6704, 2008.
52. B. Dybiec. Current inversion in the Lévy ratchet. *Physical Review E*, 78(6):061120, 2008.
53. B. Dybiec, E. Gudowska-Nowak, and I. M. Sokolov. Stationary states in Langevin dynamics under asymmetric Lévy noises. *Physical Review E*, 76:041122, 2007.
54. B. Dybiec and E. Gudowska-Nowak. Bimodality and hysteresis in systems driven by confined Lévy flights. *New Journal of Physics*, 9:452, 2007.
55. P. Reimann. Brownian motors: noisy transport far from equilibrium. *Physics Reports*, 361(2-4):57–265, 2002.
56. B. Dybiec, E. Gudowska-Nowak, and I. M. Sokolov. Transport in a Lévy ratchet: Group velocity and distribution spread. *Physical Review E*, 78:011117, 2008.
57. M. Vlad, F. Spineanu, and S. Benkadda. Impurity pinch from a ratchet process. *Physical Review Letters*, 96(8):085001, 2006.
58. R. Phillips and S. R. Quake. The biological frontier of physics. *Physics Today*, 59:38–43, 2006.
59. V. V. Uchaikin and V. M. Zolotarev. *Chance and stability. Stable distributions and their applications*. Modern Probability and Statistics. VSP, 1999.
60. A. Janicki and A. Weron. *Simulation and chaotic behaviour of  $\alpha$ -stable stochastic processes*, volume 178 of *Pure and Applied Mathematics*. Marcel Dekker, Inc., 1994.
61. A. Janicki. *Numerical and Statistical Approximation of Stochastic Differential Equations with non-Gaussian Measures*. Hugo Steinhaus Centre for Stochastic Methods, Wrocław, 1996.
62. B. Dybiec and E. Gudowska-Nowak. Resonant activation driven by strongly non-Gaussian noises. *Fluctuation and Noise Letters*, 4(2):L273–L285, 2004.
63. B. Dybiec, E. Gudowska-Nowak, and P. Hänggi. Lévy-Brownian motion on finite intervals: Mean first passage time analysis. *Physical Review E*, 73(4):046104, 2006.